



## Original Article

# Expression of polydom in dermal neurofibroma and surrounding dermis in von Recklinghausen's disease



Tomo Kamitani<sup>a</sup>, Hiroyuki Murota<sup>a,b,\*</sup>, Noriko Arase<sup>a</sup>, Mari Wataya-Kaneda<sup>a</sup>, Ryoko Sato-Nishiuchi<sup>c</sup>, Kiyotoshi Sekiguchi<sup>c</sup>, Daisuke Okuzaki<sup>d</sup>, Daisuke Motooka<sup>d</sup>, Ichiro Katayama<sup>a,e</sup>

<sup>a</sup> Dermatology, Department of Integrated Medicine, Graduate School of Medicine, Osaka University, Osaka, Japan

<sup>b</sup> Department of Dermatology, Nagasaki University Graduate School of Biomedical Sciences, Nagasaki, Japan

<sup>c</sup> Division of Matrixome Research and Application, Institute for Protein Research, Osaka University, Osaka, Japan

<sup>d</sup> Genome Information Research Center, Research Institute for Microbial Diseases, Osaka University, Osaka, Japan

<sup>e</sup> Department of Pigmentation Research and Therapeutics Graduate School of Medicine, Osaka City University, Osaka, Japan

## ARTICLE INFO

## Article history:

Received 3 December 2018

Received in revised form 6 August 2019

Accepted 12 September 2019

## Keywords:

von Recklinghausen's disease

Neurofibroma

Polydom

Platelet-derived growth factor B

TGF- $\beta$

## ABSTRACT

**Background:** Neurofibromas in von Recklinghausen's disease (vRD) can develop in the dermis. Therefore, we hypothesized that a dermal niche exists that promotes the development of these neurofibromas in subjects with vRD.

**Objective:** The purpose of this study is to examine the function of polydom, known as a ligand for integrin, mediating cell adhesion, and expressed in mouse nerve tissue, in promotion of neurofibroma.

**Methods:** Molecular, transcriptome and immunohistochemical analysis were performed to investigate the association between polydom expression and neurofibroma development.

**Results:** Polydom mRNA levels were significantly higher in neurofibroma tissue than in control tissue. Quantitative reverse transcription-polymerase chain reaction (qRT-PCR) analysis of RNA purified from primary cultured dermal neurofibroma cells demonstrated significantly higher polydom mRNA expression in cells derived from the surrounding dermis of neurofibromas compared to those from normal human dermal fibroblasts. RNA sequencing was used to compare gene expression between cultured cells derived from dermal neurofibroma-surrounding tissue with or without polydom knockdown. Subsequent gene ontology assays revealed that expression of *integrin $\beta$ 8* (*ITGB8*), a factor that releases transforming growth factor- $\beta$  (TGF- $\beta$ ) from pro-TGF- $\beta$ , was downregulated following polydom knockdown, suggesting upregulation of polydom-mediated TGF- $\beta$  production. Furthermore, we observed a strong association between polydom expression and the increase in platelet-derived growth factor B (*PDGFB*) expression in primary cultured cells from the surrounding dermis of neurofibromas exposed to TGF- $\beta$ 1.

**Conclusion:** Our results suggest that increased polydom expression in the dermis surrounding neurofibromas may promote dermal neurofibroma development by activating the TGF- $\beta$  signaling pathway.

© 2019 Published by Elsevier B.V. on behalf of Japanese Society for Investigative Dermatology.

## 1. Introduction

vRD is one of the most common monogenic diseases. Dermal neurofibromas considerably worsen patient quality of life in many

ways; thus, establishing promising treatments is an urgent issue. The only effective treatment is repeated surgery, but new tumors continuously develop. Conservative treatment for these tumors is not established. Dermal neurofibromas derive from Schwann cells [1–4], but the mechanism of this phenomenon is poorly understood. An understanding of how neurofibromas develop is needed to elucidate their pathophysiology and identify less invasive treatments and prophylaxis.

Several studies have examined the mechanisms of neurofibroma development. Liao et al isolated skin-derived precursors (SKP), which exist in dermis and have similar characteristics to stem cells [5]. When SKPs are transplanted to the sciatic nerve of mice, neurofibromas develop. These results demonstrate that

**Abbreviations:** vRD, von Recklinghausen's disease; NF1, neurofibromatosis type 1; NF, neurofibroma; NHDF, normal human dermal fibroblast; siRNA, small interfering RNA; ITGB8, integrin $\beta$ 8; TGF- $\beta$ , transforming growth factor- $\beta$ ; PDGFB, platelet-derived growth factor B; EsR, estrogen receptor; PrR, progesterone receptor.

\* Corresponding author at: Department of Dermatology, Nagasaki University, 1-7-1 Sakamoto, Nagasaki, 852-8501, Japan.

E-mail address: [h-murota@nagasaki-u.ac.jp](mailto:h-murota@nagasaki-u.ac.jp) (H. Murota).

neurofibroma development requires both mutation of the neurofibromatosis type 1 (NF1) gene and an ideal microenvironment including peripheral nerves. They also suggested that factors secreted from peripheral nerve tissue are needed to induce neurofibromas, and interactions between Schwann cells and the surrounding nerve may be a treatment target. Wu et al demonstrated that the Nf1-Stat3-Arid1b/ $\beta$ -catenin pathway, in the context of Nf1 loss, has an important role in neurofibroma development in the mouse model [6]. In addition, generation of tumors mediated by Stat3 activation has been reported in other organs and tissues [7]. However, the factors related to the mechanism of neurofibroma generation remains obscure.

In this study, we focused on polydom that is expressed in the nerve tissue of mice [8]. We show that polydom is specifically expressed in the surrounding dermis of neurofibromas. RNA sequence analysis revealed that polydom in the dermis might activate integrin $\beta$ 8 (ITGB8).

ITGB8 is a 100-kDa glycoprotein that heterodimerizes exclusively with the 130-kDa  $\alpha$ v subunit [9,10]. ITGB8 silencing changes lung cancer cells to a less invasive phenotype [11]. Polydom is reported to be biomarker which can be used for diagnosis of metastatic lung cancer in pleural effusion [12]. Based on these facts, polydom and ITGB8 may play an important role in the development of lung cancer. Therefore, we hypothesized that ITGB8 plays an important role in neurofibroma development.

The integrin family including ITGB8 binds to pro-transforming growth factor (TGF)- $\beta$ 1, which releases TGF- $\beta$ 1 leading to activation of TGF- $\beta$  signaling [13]. In addition, both TGF- $\beta$  and platelet-derived growth factor B (PDGFB) are key factors in the development of neurofibromas in patients with NF1 [14]. Based on our

results and this knowledge, we conclude that increased polydom expression in the dermis surrounding neurofibromas elevates ITGB8 expression, leading to activation of the TGF- $\beta$  signaling pathway and promoting neurofibroma development.

## 2. Material and methods

### 2.1. Human specimens

Human surgery samples were obtained from patients with NF1 and patients with control tumors. All participants provided written informed consent. All studies were approved by the ethical committee of Osaka University. Detailed patient demographic characteristics (e.g., age, sex, surgery site) are described in Table 1.

### 2.2. Cell culture

#### 2.2.1. Primary cultured fibroblasts were used in this study

We divided the surgical specimens of neurofibromas into macroscopically clear and elastic parts and non-glossy and nonelastic parts. We classified the former parts as tumor tissue, and the latter parts as normal tissue. Tissues containing both shiny and non-shiny parts were discarded. Normal tissue surrounding neurofibromas or neurofibroma tumors were cut into pieces, placed on culture plates (Corning, Corning Inc., NY, USA) with media, and incubated for several weeks at 37 °C in a 5% CO<sub>2</sub> atmosphere. When they reached confluency, the cells were harvested using trypsin/EDTA (Nacalai Tesque, Kyoto, Japan) solution and further passaged. The cells were incubated in the same atmosphere and used for experiments.

**Table 1**

Clinical features of NF1 (1–27) and control patients (28–35). T: tumor; D: dermis; N.D.: not done; NF1: neurofibromatosis type 1.

case	age (years)	sex	disease	location	stained by polydom(T)	stained by polydom(D)	expression of polydom (primary cultured tumor cells)	expression of polydom (primary cultured dermis cells)	serum estradiol (pg/ml)
1	13	male	NF1	trunk	–	±	N.D.	N.D.	N.D.
2	20	male	NF1	unknown	–	±	N.D.	N.D.	N.D.
3	36	male	NF1	lower limb	–	±	N.D.	N.D.	N.D.
4	38	male	NF1	lower limb	–	±	N.D.	N.D.	N.D.
5	46	male	NF1	upper limb	–	±	0.427	0.845	N.D.
6	48	male	NF1	trunk	–	±	0.126	0.042	N.D.
7	52	male	NF1	trunk	–	±	N.D.	N.D.	35
8	52	male	NF1	trunk	–	±	N.D.	N.D.	N.D.
9	57	male	NF1	trunk	–	+	N.D.	N.D.	47
10	57	male	NF1	trunk	N.D.	N.D.	N.D.	N.D.	N.D.
11	57	male	NF1	upper limb	N.D.	N.D.	0.774	1.703	33.7
12	74	male	NF1	upper limb	–	+	N.D.	N.D.	N.D.
13	24	female	NF1	trunk	–	±	0.4	8.781	36.7
14	26	female	NF1	trunk	N.D.	N.D.	0.088	0.094	63.4
15	30	female	NF1	lower limb	–	±	N.D.	N.D.	N.D.
16	36	female	NF1	trunk	–	±	N.D.	N.D.	N.D.
17	37	female	NF1	unknown	N.D.	N.D.	0.1	0.366	N.D.
18	42	female	NF1	trunk	–	±	N.D.	N.D.	N.D.
19	43	female	NF1	lower limb	–	±	0.864	0.022	N.D.
20	49	female	NF1	upper limb	N.D.	N.D.	0.057	0.027	N.D.
21	50	female	NF1	unknown	–	±	0.248	0.115	335
22	54	female	NF1	trunk	N.D.	N.D.	0.161	0.339	N.D.
23	55	female	NF1	upper limb	N.D.	N.D.	0.021	1.87	N.D.
24	56	female	NF1	lower limb	–	±	N.D.	N.D.	<14.0
25	57	female	NF1	trunk	–	±	0.735	0.004	N.D.
26	63	female	NF1	lower limb	–	±	0.255	0.113	N.D.
27	69	female	NF1	lower limb	–	±	0.998	3.667	17.8
28	63	male	soft fibroma	lower limb	N.D.	N.D.	N.D.	N.D.	N.D.
29	37	male	normal	trunk	N.D.	±	N.D.	N.D.	N.D.
30	68	male	normal	trunk	N.D.	±	N.D.	N.D.	N.D.
31	69	male	normal	upper limb	N.D.	±	N.D.	N.D.	N.D.
32	50	female	fibrokeratoma	upper limb	N.D.	N.D.	N.D.	N.D.	N.D.
33	44	female	dermatofibroma	lower limb	N.D.	N.D.	N.D.	N.D.	N.D.
34	66	female	normal	trunk	N.D.	+	N.D.	N.D.	N.D.
35	67	female	normal	trunk	N.D.	±	N.D.	N.D.	N.D.

### 2.3. Small interfering RNA (siRNA) transfection

Primary cultured cells from the surrounding dermis of neurofibromas ( $8 \times 10^4/1.5$  ml) were seeded onto 6-well dishes 1 day prior to transfection. Cells were transfected with 30 nM polydom siRNA with 4 different sequences (Hs\_SVEP1\_5; target sequence; 5'-AAGGGTCTACTGACAAGTATT-3', Hs\_SVEP1\_6; target sequence; 5'-CAGGGCCCTCCATTATTGAA-3', Hs\_SVEP1\_7; target sequence; 5'-CTGGCCGGTGATAAAGAATCA-3', Hs\_SVEP1\_8; target sequence; 5'-CTCGTGACTATTACCAACCTA-3', QIAGEN, Hilden, Germany) or control siRNA (Target sequence is not disclosed) (AllStars Negative Control siRNA, QIAGEN, Hilden, Germany) using RNAi MAX (Invitrogen, Carlsbad, California, USA). The culture medium was replaced 6 h later. One day after transfection, total RNA was purified as described below.

We performed preliminary experiments using an siRNA with four different sequences (Hs\_SVEP1\_5, Hs\_SVEP1\_6, Hs\_SVEP1\_7, and Hs\_SVEP1\_8) and found that Hs\_SVEP1\_8 was the most effective than other conceivable combination of siRNAs by western blot analysis. Therefore, we used only one siRNA for polydom knockdown in our later experiment.

### 2.4. Expression and purification of recombinant human SVEP1 protein

DNA segments encoding human SVEP1 (amino acids 18–3571) were obtained by RT-PCR using human placenta total RNA (Clontech, Mountain View, CA). The cDNA fragments were inserted into pSec-NFLAG-His [8] at the BamHI/NotI sites, using GeneArt™ Seamless Cloning and Assembly Kit (Thermo Fisher Scientific). Recombinant SVEP1 proteins were produced using Freestyle 293 Expression System (Invitrogen), and purified using anti-FLAG M2-agarose (Sigma), as described previously [8].

### 2.5. Immunoblotting

siRNA transfected fibroblasts were lysed as previously described (inyo). The lysates were separated by SDS/PAGE and were blotted with anti-polydom c-terminal pAb, followed by Stabilized Goat Anti-Rabbit HRP-Conjugated (Thermo Scientific). Peroxidase activity was detected with the SuperSignal reagent (Thermo Scientific), as described previously [15].

### 2.6. RNA isolation from primary cultured cells and quantitative real-time PCR (RT-qPCR)

Total RNA was extracted from primary cultured cells treated for 6 h with mock, 5 ng/ml  $\beta$ -estradiol (SIGMA-ALDRICH, St. Louis, Missouri, USA), 10 ng/ml TGF- $\beta$ 1 (R&D SYSTEMS, Minneapolis, Minnesota, USA), or siRNA (QIAGEN) using the Maxwell 16 LEV simply RNA Tissue kit (Promega, Madison, Wisconsin, USA). First-strand cDNA was synthesized using ReverTra Ace qPCR RT Master Mix (TOYOBO, Osaka, Japan) according to the manufacturer's protocol. PCR was performed using THUNDERBIRD SYBR qPCR Mix (TOYOBO) and the QuantStudio7 Flex (Applied Biosystems, Foster City, California, USA), 7900 HT Sequence Detection System (Applied Biosystems), or 7900 HT Fast Real-Time PCR system (Applied Biosystems). The quantity of each transcript was determined using the standard curve method and normalized to the expression of glyceraldehyde-3-phosphate dehydrogenase (GAPDH).

### 2.7. RNA isolation from tissue samples

Tissue samples were submerged in RNAlater (Invitrogen) and stored at  $-80^\circ\text{C}$  until use. Total RNA was extracted from the tissue using a Tissue Ruptor (QIAGEN) and RNeasy Fibrous Tissue Mini Kit (QIAGEN) according to the manufacturer's protocol.

### 2.8. RNA sequencing and pathway analysis

RNA sequencing was performed for polydom knockdown cells and normal cells. Library preparation was performed using a TruSeq stranded mRNA sample prep kit (Illumina, San Diego, CA) according to the manufacturer's instructions. Sequencing was performed on an Illumina HiSeq 2500 platform in a 75-base single-end mode. Illumina Casava1.8.2 software was used for base calling. Sequenced reads were mapped to the human reference genome sequences (hg19) using TopHat v2.0.13 in combination with Bowtie2 ver. 2.2.3 and SAMtools ver. 0.1.19. The fragments per kilobase of exon per million mapped fragments (FPKM) were calculated using Cufflinks ver.2.2.1. The raw data were deposited in the NCBI's Gene Expression Omnibus database (GSE117322). A final series of differentially expressed genes with fold change  $> 2.0$  and  $p$ -value  $< 0.05$  was identified for further analysis.  $P$ -values were derived from paired  $t$ -tests in polydom knockdown and negative control conditions. Genes downregulated by knockdown of polydom were identified with the Illumina Correlation Engine.

### 2.9. Histopathological analysis

For immunostaining of S100, paraffin-embedded skin sections (5- $\mu\text{m}$  thick) were processed using heat-mediated antigen retrieval for 15 min at  $120^\circ\text{C}$  in Tris-EDTA buffer, pH 9.0. Sections were incubated with the primary antibody (rabbit anti-S100 antibody, Abcam, Cambridge, UK) for 1 h at room temperature. After washing with Tris-buffered saline (TBS) containing 0.05% Triton-X100, the slides were mounted using the Vectastain ABC kit (Vector Laboratories, Burlingame, CA, USA).

For immunostaining of other protein, paraffin-embedded skin sections (5- $\mu\text{m}$  thick) were processed using heat-mediated antigen retrieval for 10 min at  $120^\circ\text{C}$  in citrate buffer, pH 6.0. Sections were incubated with primary antibodies overnight at  $4^\circ\text{C}$ , secondary antibodies for 1 h at room temperature, followed by nuclear staining (Hoechst 33342, ThermoFisher Scientific, Waltham, Massachusetts, USA).

Cells were plated in the Lab-Tek Chamber Slide System (ThermoFisher Scientific) and after 24 h were fixed in 4% paraformaldehyde phosphate buffer solution. The slides were then incubated with antibodies followed by nuclear staining as done for paraffin-embedded skin sections.

The primary antibodies used in this study were polyclonal rabbit anti-polydom (dilution, 2  $\mu\text{g}/\text{mL}$ , Division of Matrixome Research and Application, Institute for Protein Research, Osaka University, Suita, Osaka, Japan), monoclonal mouse anti-vimentin (ready-to-use, Dako, Glostrup, Denmark), polyclonal rabbit anti-estrogen receptor beta (dilution, 1:200, Abcam, Cambridge, UK), and polyclonal rabbit anti-progesterone receptor (dilution, 1:200, Abcam). The secondary antibodies were Alexa Flour 488-conjugated goat anti-rabbit IgG (dilution, 1:400, ThermoFisher Scientific), Alexa Flour 555-conjugated goat anti-mouse IgG (dilution, 1:400, ThermoFisher Scientific), and Polyclonal Swine Anti-Rabbit Immunoglobulins fluorescein isothiocyanate (dilution, 1:5,000, Dako). Images were acquired using a fluorescence microscope (BZ-9000, Keyence, Osaka, Japan). For the ratio of polydom-positive cells, fluorescence images were converted to gray-scale images, and mean gray values were calculated using ImageJ software (National Institutes of Health, Baltimore, Maryland, USA). Vimentin- and polydom-positive areas were defined as a fluorescence intensity above a threshold and quantified using a BZ analyzer (Keyence).

### 2.10. Statistical analysis

Statistical analysis was performed using GraphPad Prism (La Jolla, California, USA). Data were analyzed using two-tailed

unpaired t-tests. P-values < 0.05 were considered statistically significant.

### 3. Results

#### 3.1. Increased *polydom* mRNA expression in neurofibroma tissue and primary cultured neurofibroma cells

We first confirmed the pathological diagnosis of neurofibromas in specimen used in this study (Fig. 1A). Next, we

investigated *polydom* mRNA expression in both tumors and the surrounding normal tissues. Normal tissue and neurofibroma tumors were preserved separately. We performed immunostaining of paraffin-embedded sections of tumor and surrounding dermis for S100, and found tumor section was well stained by S100 antibody, whereas dermis section was not stained (Fig. 1B), indicating that normal tissue and neurofibroma tumors were clearly separated. Then, total RNA was extracted for qRT-PCR. The relative expression of *polydom* was calculated and was used to compare its expression level between neurofibroma and healthy

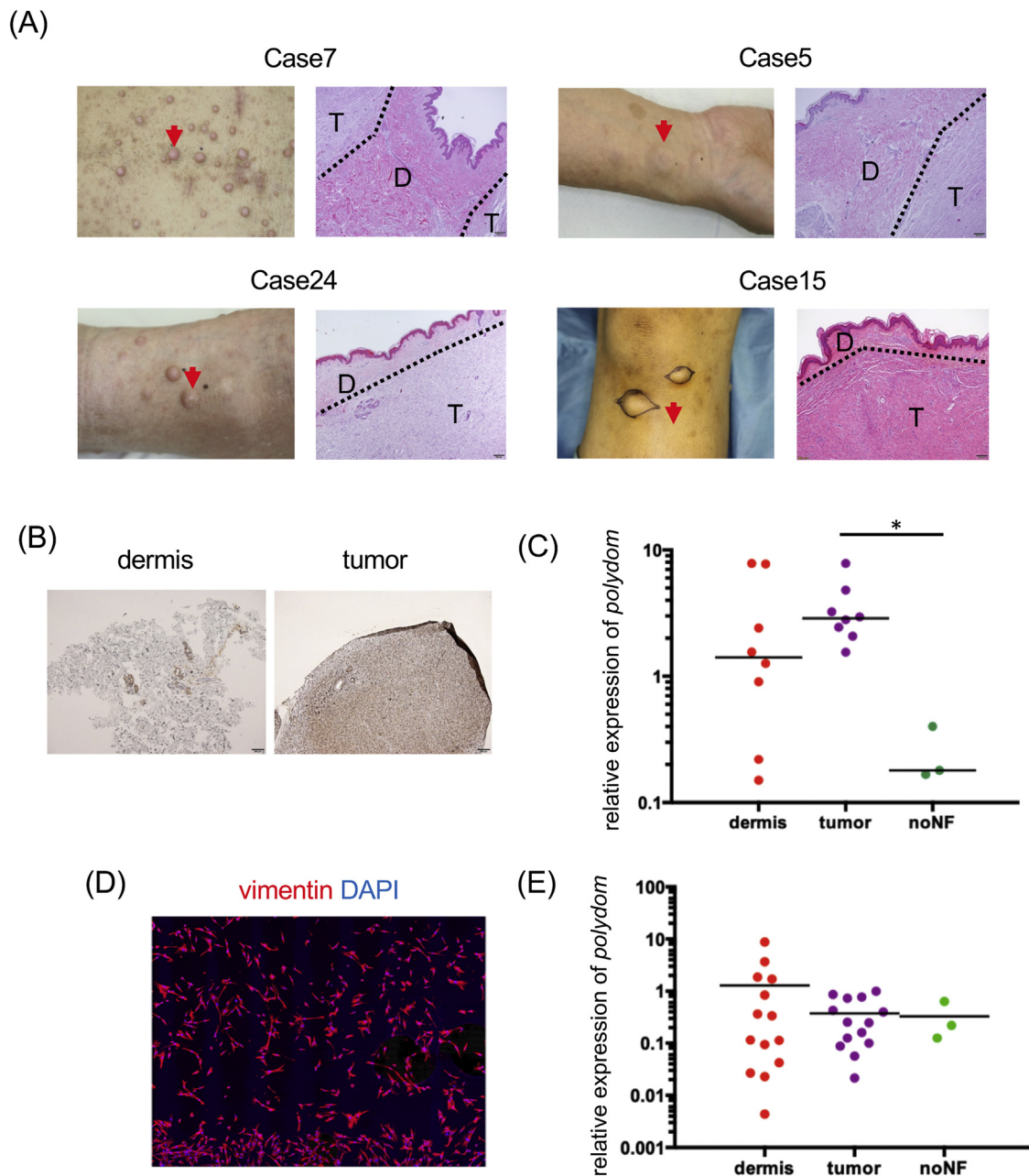


**Fig. 1.** Expression of *polydom* mRNA in neurofibroma tissue and primary cultured neurofibromas.

(A) Clinical findings and histopathology of the patients who provided each sample. T: tumor, D: dermis.

(B) Paraffin-embedded sections of tumor and surrounding dermis were stained for S100 (case 24).

(C) Expression of *polydom*/*GAPDH* in the surrounding dermis of neurofibromas and tumor tissue of neurofibromas (cases 5, 6, 7, 9, 13, 18, 21, 27), and control tissue (cases 28, 33, 34). Bars indicate mean value. \* means significant difference (p-value < 0.05).

(D) Immunocytochemistry of primary cultured cells from the surrounding dermis of a neurofibroma (case 8).

(E) Expression of *polydom* mRNA in primary cultured neurofibromas (cases 5, 6, 11, 13, 14, 17, 19–23, 25–27) and normal human dermal fibroblasts. Total RNA was purified for qRT-PCR from normal human dermal fibroblasts, primary cultured cells from the surrounding dermis of neurofibromas, and cells from the tumor itself. Bars indicate mean value.

dermal tissue. Intriguingly, tumor and tumor surrounding tissue from six to eight subjects with neurofibroma showed approximately 3.6–31.4 times higher *polydom* expression than control dermal tissues (Fig. 1C).

We also examined *polydom* expression in primary cultured cells from tumor-surrounding normal tissue and tumors. Immunocytochemistry suggested that cells from normal tissue surrounding neurofibromas had characteristics of fibroblasts (Fig. 1D). In four samples of dermal cells of neurofibromas showed approximately 5.2–26.8 times higher expression compared to noNF (Fig. 1E), although there was no significant difference. These results suggest that *polydom* expression maintained in some subjects with neurofibromas, especially in fibroblasts from normal tissue surrounding neurofibromas in vitro culture.

We also performed immunostaining of paraffin-embedded sections of neurofibromas and normal tissue. Although *polydom*-positive fibroblasts were seen in the surrounding dermis of neurofibromas, the number of *polydom*-positive fibroblasts varied widely among all study subjects (Supplementary Fig. 1).

Next, we examined why *polydom* was produced in the neurofibromas and surrounding tissues of neurofibromas. Sex hormones may play an important role in increasing *polydom*

expression and facilitating neurofibroma development because they often arise after puberty, although estradiol concentrations in the serum of NF1 patients were not increased (Table 1). In our daily medical examination, we found that there are more female patients than male patients with NF1 in our clinic (42 male and 54 female patients), although there was no statistically difference. In addition, it is recently said that there may be a role of sex hormones in development of dermal neurofibromas [16]. Based on this, we hypothesized that female hormones promote *polydom* expression. To test this, we performed histopathological analysis of immunofluorescence-labeled paraffin-embedded sections to examine estrogen receptor and progesterone receptor levels (Supplementary Fig. 2). Compared with normal sections, the expression of these receptors was not increased in either the dermis or tumor tissue.

We also investigated the influence of  $\beta$ -estradiol on *polydom* expression in primary cultured cells (Supplementary Fig. 3). The cells were cultured for 6 h with or without 5 ng/ml  $\beta$ -estradiol. Total RNA was purified from these cells to perform qRT-PCR for *polydom*. The influence of  $\beta$ -estradiol did not show a clear trend, suggesting that sex hormones are unrelated to increased *polydom* expression.

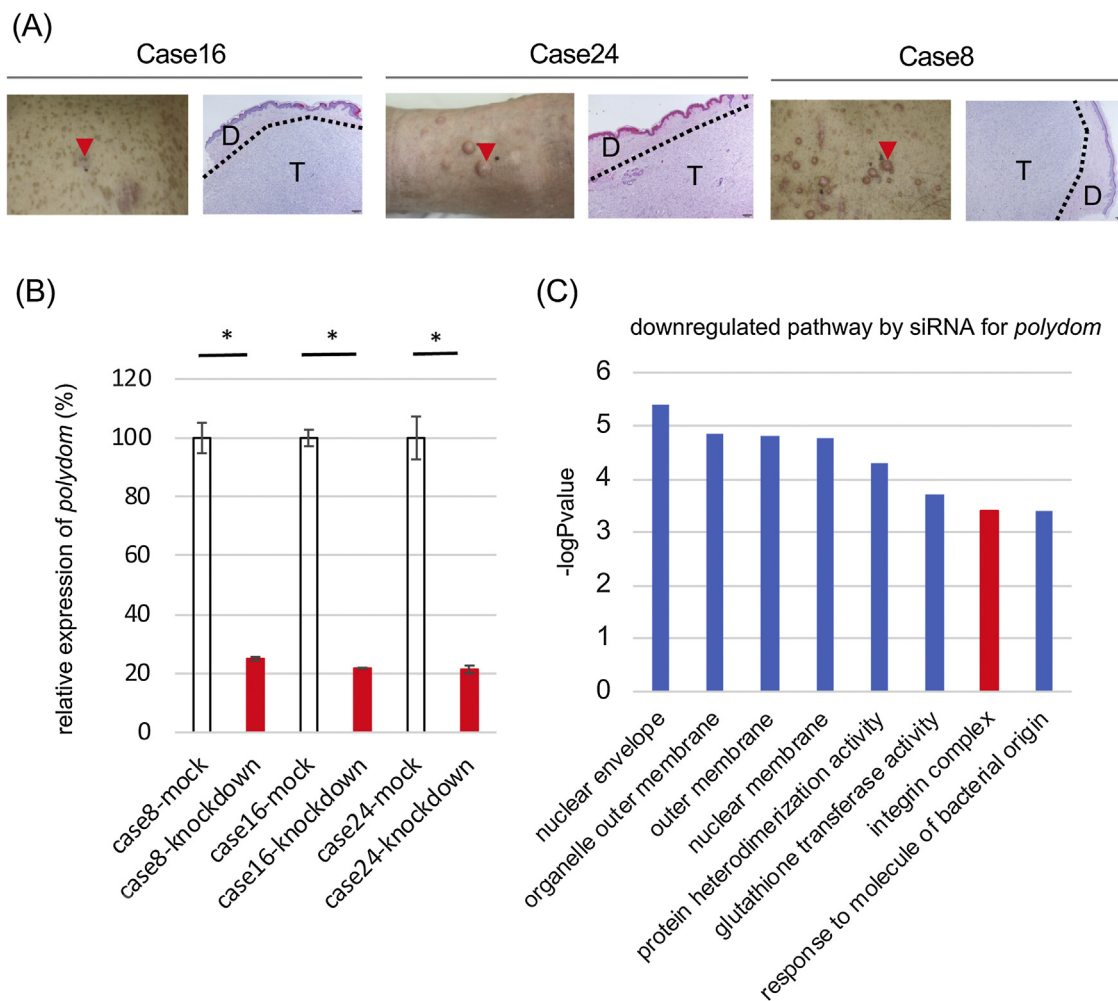


**Fig. 2.** RNA sequencing and gene ontology assay.

(A) Clinical findings and histopathology of the patients who provided each sample. T: tumor. D: dermis.

(B) mRNA of *polydom* in primary cultured cells from surrounding dermis of neurofibromas.

(cases 8, 16, 24) was knocked down by siRNA. Total RNA was purified from the cells. The decrease in mRNA of *polydom* was confirmed by qRT-PCR. \* means significant difference (p-value < 0.05).

(C) Total RNA was used for gene ontology assays.

### 3.2. Polydom promotes integrin $\beta$ 8 expression and increases in TGF $\beta$ 1 and PDGFB

We next investigated the downstream pathway of polydom in fibroblasts surrounding neurofibromas. To achieve this objective, we knocked-down *polydom* in primary cultured fibroblasts from the surrounding dermis of neurofibromas (Fig. 2A) using small

interfering RNA (Fig. 2B). We confirmed that amount of polydom protein was reduced to 36% one day after transfection by immunoblotting (Fig. 2C). Then, we performed transcriptome analysis using RNA sequencing (Fig. 2D, Supplementary Fig. 4, Supplementary Table S2-3). Using a gene ontology assay from Illumina Correlation Engine (Illumina, San Diego, California, USA), a decrease in the expression of factors such as those related to the

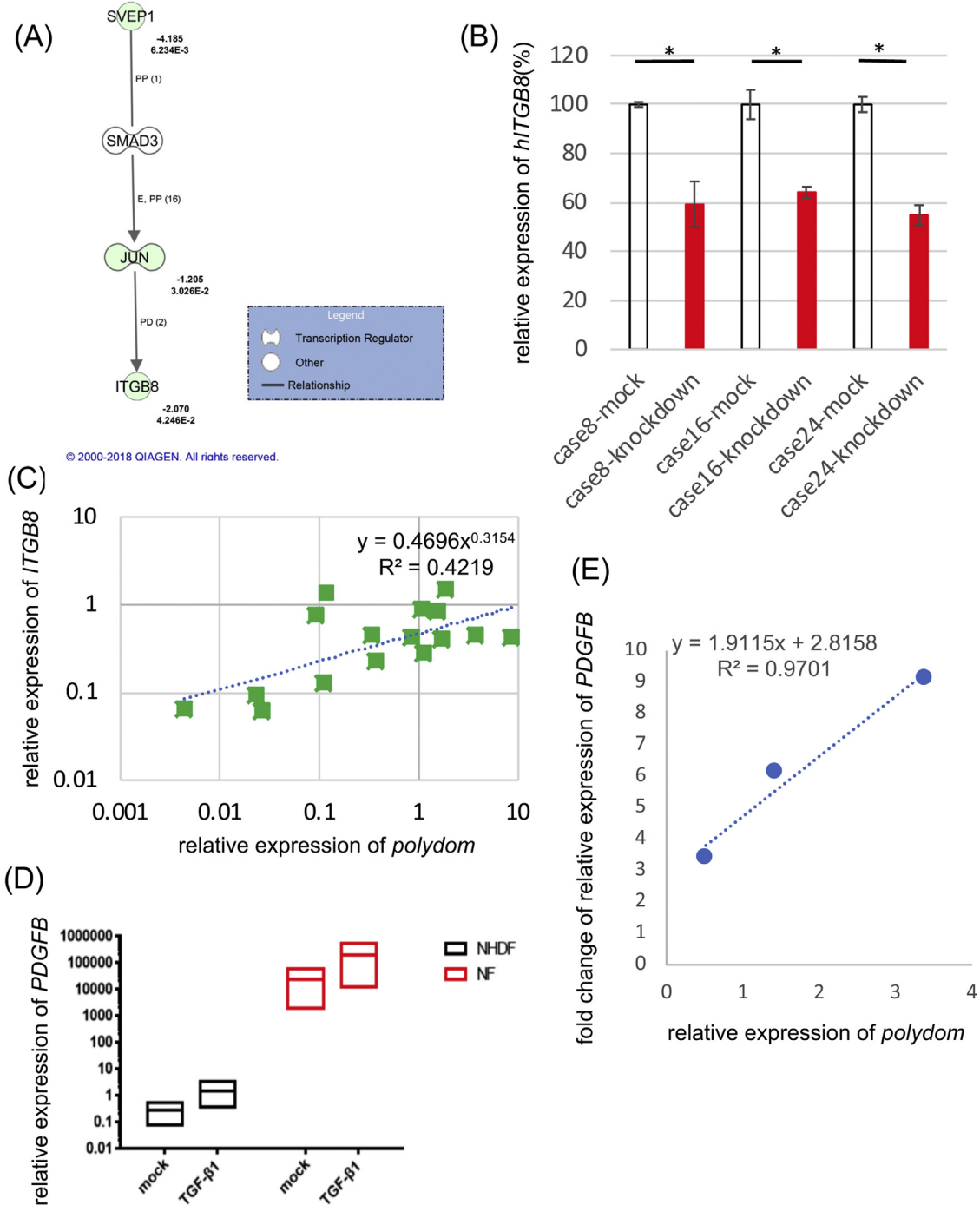


**Fig. 3.** Downstream pathway analysis.

(A) Downstream pathway of polydom.

(B) Expression of *integrin $\beta$ 8*. qRT-PCR using total RNA (Fig. 2B) revealed lower *integrin $\beta$ 8* expression in knockdown cells compared to control cells. Error bars mean  $\pm$  standard deviation. \* means significant difference (p-value < 0.05).

(C) Comparison of *polydom* and *ITGB8* expression in primary cultured dermis cells (cases 6, 8, 11, 13, 14, 16, 17, 19, 20–27). The correlation between expression levels is shown.

(D) Normal human dermal fibroblasts and primary cultured dermis cells (cases 8, 10, 16) were treated with TGF- $\beta$ 1 or mock (treatment with vehicle). qRT-PCR using total RNA for *PDGFB* revealed stronger *PDGFB* expression in primary cultured dermis cells, and higher expression in the presence of TGF- $\beta$ 1.

(E) Comparison of *polydom* expression in primary cultured dermis cells (case 8, 10, 16) and fold change of relative expression of *PDGFB* induced by TGF- $\beta$ 1.

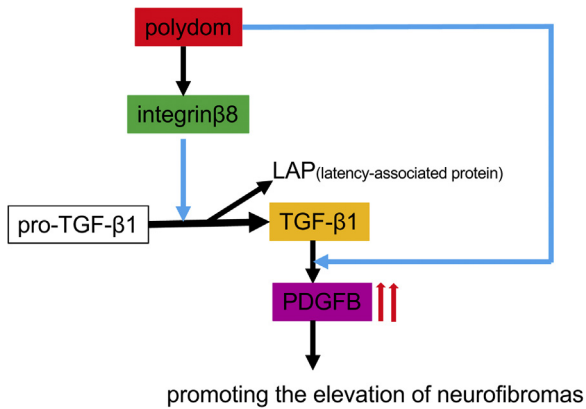


**Fig. 4.** Hypothesis.

Increased polydom expression in the dermis leads to increased integrin $\beta$ 8, resulting in higher TGF- $\beta$ 1 levels, which leads to increased PDGFB. Polydom also facilitates the production of PDGFB mediated by TGF- $\beta$ 1, and promotes neurofibroma development.

nuclear envelope, outer membrane, and integrin complex was seen when expression of *polydom* was reduced. Within the integrin complex, *integrin $\beta$ 8* was markedly downregulated after *polydom* knockdown (Fig. 3A and Supplementary Fig. 4). We confirmed the decrease of *integrin $\beta$ 8* expression by downregulation of *polydom* using qRT-PCR (Fig. 3B).

We found relationship between *polydom* and *ITGB8* expression in primary cultured cells from the surrounding dermis of neurofibromas (Fig. 3C). Next, we assessed the influence of TGF- $\beta$ 1 on *PDGFB* expression, a key factor in neurofibroma development [14]. In the presence of TGF- $\beta$ 1, *PDGFB* expression was increased in both NHDF and primary cultured cells from the surrounding dermis of neurofibromas, but baseline expression was 79,100 times higher in primary cultured cells than in NHDF (Fig. 3D). Next, we investigated the relationship between *polydom* expression in primary cultured cells and fold change of relative expression of *PDGFB* induced by TGF- $\beta$ 1 (Fig. 3E). Interestingly, there was a strong association between *polydom* and the increase in *PDGFB*. These results suggest that polydom increases *ITGB8* expression and the subsequent increases of activated TGF- $\beta$ 1, whereas polydom also promotes the production of PDGFB mediated by TGF- $\beta$ 1, ultimately facilitating neurofibroma development (Fig. 4).

#### 4. Discussion

Polydom is an extracellular matrix protein that is a ligand for integrin. This > 3500-amino acid protein is composed of an N-terminal signal sequence and an array of domains characteristic of extracellular matrix [8]. Sato-Nishiuchi et al reported that polydom is localized at the submucosal mesenchyme in the stomach and intestine, sinusoids in the liver, Bowman's capsules, and the mesenchyme between renal tubules in the kidney, as well as the lung mesenchyme in mice embryos [8]. They also found that polydom is strongly expressed in mouse nerve tissue. Other researchers reported that polydom is expressed in both breast and lung cancers [12,17]. Because polydom is highly expressed in mouse nerve tissue or human cancer tissue, we assessed the possibility that polydom may play an important role in neurofibroma formation.

Although polydom-positive fibroblasts were seen in the surrounding dermis of neurofibromas, the number of polydom-positive fibroblasts varied widely among all study subjects (Supplementary Fig. 1). We estimate that intensity of signal of polydom tended to be weaker than previous report because we used antibody for murine polydom [8]. Furthermore, it seemed to

be difficult to precisely quantitate polydom levels using paraffin sections by immunostaining, because it is secretory protein. Accordingly, we analyzed mRNA expression of *polydom* in situ. Neurofibroma tissue strongly expressed *polydom* mRNA (Fig. 1C). In addition, there was abundant *polydom* expression in primary cultured cells from the surrounding dermis of neurofibromas (Fig. 1E). Stromal fibroblasts in invasive human breast carcinomas are known to promote tumor growth [18]. Considering these facts, polydom-positive fibroblasts may accelerate neurofibroma development.

We explored why polydom was increased in the surrounding dermis of neurofibromas. Dermal neurofibromas in patients with NF1 usually begin to develop at puberty and after. Polydom is regulated in an estrogen-dependent manner in breast cancer cells [19]. These facts suggested that sex hormones regulate *polydom* mRNA expression in the surrounding dermis of neurofibromas. In contradiction to this hypothesis, estradiol concentrations in the serum of NF1 patients were not increased (Table 1). There were also no increases in serum estriol or progesterone concentrations (data not shown). We next assayed *polydom* mRNA in primary cultured cells from tumors and surrounding dermis after  $\beta$ -estradiol treatment, but *polydom* expression was not significantly different (Supplementary Fig. 3). Shur et al reported a biphasic effect, showing increased polydom expression in proliferating cells challenged with  $\beta$ -estradiol and decreased polydom in confluent cells [19]. We consider that we observed different patterns because we seeded primary cultured cells with varying rates of proliferation to examine the effect of  $\beta$ -estradiol.

To investigate the interaction between polydom and other factors, siRNA was used to knockdown *polydom* in primary cultured cells derived from the surrounding dermis of neurofibromas. Transcriptome analysis using RNA sequencing was performed (Fig. 2, Supplementary Fig. 4, Supplementary Table S2-3), and results were examined with gene ontology analysis. Pathways including the pathway of the nuclear envelope, organelle outer membrane, outer membrane, nuclear membrane, protein heterodimerization activity, glutathione transferase activity, integrin complex, and response to molecule of bacterial origin were downregulated after *polydom* knockdown. We focused on the integrin complex because polydom is a ligand for integrin, and found downregulation of *ITGB8*.

*ITGB8* is a 100-kDa glycoprotein that heterodimerizes exclusively with the 130-kDa  $\alpha$ v subunit [9,10]. *ITGB8* silencing changes lung cancer cells to a less invasive phenotype [11]. Polydom is reported to be biomarker which can be used for diagnosis of metastatic lung cancer in pleural effusion [12]. Therefore, we hypothesized that *ITGB8* plays an important role in neurofibroma development. Munger et al reported that latent TGF- $\beta$  binds to *ITGB8*, and TGF- $\beta$  can be released from latency-associated peptide and then initiate signaling via TGF- $\beta$  receptors [13]. Glioblastoma stem cells exploit the  $\alpha$ v $\beta$ 8 integrin-TGF- $\beta$ 1 signaling axis to drive tumor initiation and progression [20]. On the other hand, Kadono et al reported that PDGFB and TGF- $\beta$  play a role in neurofibroma development in NF1 [14]. We found relationship between *polydom* and *ITGB8* expression in primary cultured cells derived from the surrounding dermis of neurofibromas (Fig. 3C). Thus, polydom may activate *ITGB8* and promote the increases in TGF- $\beta$ , accelerating neurofibroma development. The mechanism of why polydom expression induce the increase of *ITGB8* remains unknown. We consider that polydom binds to SMAD3 [21], promote the activation of JUN [22], and the increase of transcription of *ITGB8* [23] from our downstream pathway analysis (Fig. 3A).

PDGFB expression was strongly increased in primary cultured cells in the presence of TGF- $\beta$ 1, and baseline expression was much higher in tumor cells than in NHDF (Fig. 3D). Furthermore, we also observed a direct relationship between *polydom* expression and

fold change of relative expression of *PDGFB* induced by TGF- $\beta$ 1 (Fig. 3E). These results suggest that polydom may promote ITGB8 expression and the subsequent increases of activated TGF- $\beta$ 1. Meanwhile, polydom promotes the direct production of PDGFB mediated by TGF- $\beta$ 1.

In conclusion, polydom expressed in dermal fibroblasts harvested from NF1 patients promoted ITGB8 expression and increases in TGF- $\beta$ 1 and PDGFB, facilitating neurofibroma development. Noninvasive treatments for neurofibromas are urgently needed to improve the quality of life of NF1 patients, and polydom and ITGB8 may be ideal targets.

The limitation of this study is that the number of cases is limited because NF1 is rare diseases and we could not collect large number of samples. Another limitation was the findings of significant relationship between polydom and ITGB8 may be a limited finding to fibroblast in NF1, because we did not use normal fibroblast nor Schwann cells derived from NF1 in the current experiment. We hope that the relationship between polydom and integrins in human skin should be investigated in future studies.

## Funding

This research received a grant from the Practical research project for rare and intractable diseases from the Japan Agency for Medical Research and development (AMED) (17ek0109082h0003) (18ek0109347h0001) to M.K-W, and a grant from the Ministry of Education, Culture, Sports, Science and Technology of Japan (16k10155) to M. K-W, and a grant from KAKENHI grant number JP18K08296.

## Declaration of Competing Interest

The authors declare no conflicts of interest.

## Acknowledgments

We thank Lingli Yang and Fei Yang for helpful discussion; Ryoko Sugiyama and Maiko Sugiura for secretarial work; and Kenju Nishida, Eriko Nobuyoshi, Yumiko Fujii, and Sayaka Matsumura for research assistance.

## Appendix A. Supplementary data

Supplementary material related to this article can be found, in the online version, at doi:<https://doi.org/10.1016/j.jdermsci.2019.09.005>.

## References

- [1] K.A. White, V.J. Swier, J.T. Cain, J.L. Kohlmeyer, D.K. Meyerholz, M.R. Tanas, J. Uthoff, E. Hammond, H. Li, F.A. Rohret, A. Goeken, C.H. Chan, M.R. Leidinger, S. Umesalma, M.R. Wallace, R.D. Dodd, K. Panzer, A.H. Tang, B.W. Darbro, A. Moutal, S. Cai, W. Li, S.S. Bellampalli, R. Khanna, C.S. Rogers, J.C. Sieren, D.E. Quelle, J.M. Weimer, A porcine model of neurofibromatosis type 1 that mimics the human disease, *JCI Insight* 3 (12) (2018).
- [2] S.H. Isakson, A.E. Rizzardi, A.W. Coutts, D.F. Carlson, M.N. Kirstein, J. Fisher, J. Vitte, K.B. Williams, G.E. Pluhar, S. Dahiya, B.C. Widemann, E. Dombi, T. Rizvi, N. Ratner, L. Messiaen, A.O. Stemmer-Rachamimov, S.C. Fahrenkrug, D.H. Gutmann, M. Giovannini, C.L. Moertel, D.A. Largaespada, A.L. Watson, Genetically engineered minipigs model the major clinical features of human neurofibromatosis type 1, *Commun Biol* 1 (158) (2018).
- [3] Z. Chen, J. Mo, J.P. Brosseau, T. Shipman, Y. Wang, C.P. Liao, J.M. Cooper, R.J. Allaway, S.J.C. Gosline, J. Guinney, T.J. Carroll, L.Q. Le, Spatiotemporal loss of *NF1* in Schwann Cell lineage leads to different types of cutaneous neurofibroma susceptible to modification by the hippo pathway, *Cancer Discov.* 9 (1) (2019) 114–129.
- [4] K.J. Radomska, F. Couplier, A. Gresset, A. Schmitt, A. Debliche, S. Lemoine, P. Wolkenstein, J.M. Vallat, P. Charnay, P. Topilko, Cellular origin, tumor progression, and pathogenic mechanisms of cutaneous neurofibromas revealed by mice with *Nf1* knockout in boundary cap cells, *Cancer Discov.* 9 (1) (2019) 130–147.
- [5] C.P. Liao, S. Pradhan, Z. Chen, A.J. Patel, R.C. Booker, L. Le, The role of nerve microenvironment for neurofibroma development, *Oncotarget* 7 (38) (2016) 61500–61508.
- [6] J. Wu, V.W. Keng, D.M. Patmore, R.J. Spinner, D.A. Largaespada, N. Ratner, Insertional mutagenesis identifies a STAT3/Arid1b/ $\beta$ -catenin pathway driving neurofibroma initiation, *Cell Press* 14 (2016) 1979–1990.
- [7] K.S. Siveen, S. Sikka, R. Surana, X. Dai, J. Zhang, A.P. Kumar, B.K. Tan, G. Sethi, A. Bishayee, Targeting the STAT3 signaling pathway in cancer: role of synthetic and natural inhibitors, *Biochim. Biophys. Acta* 1845 (2) (2013) 136–154.
- [8] R. Sato-Nishiuchi, I. Nakano, A. Ozawa, Y. Sato, M. Takeichi, D. Kiyozumi, K. Yamazaki, T. Yasunaga, S. Futaki, K. Sekiguchi, Polydom/SVEP1 is a ligand for integrin  $\alpha$ 9 $\beta$ 1, *J. Biol. Chem.* 287 (30) (2012) 25615–25630.
- [9] L. Stephen, NishimuraSO, Dean Sheppard, Robert Pytela, Integrin  $\alpha$ v $\beta$ 8 interaction with vitronectin and functional divergence of the p8 cytoplasmic domain, *J Biol. Chem.* 269 (46) (1994) 28708–28715.
- [10] Kristine Venstrom, Louis Reichardt,  $\beta$ 8 integrins mediate interactions of chick sensory neurons with laminin-1, collagen IV, and fibronectin, *Mol. Biol. Cell* 6 (1995) 419–431.
- [11] Zhaoguo Xu, Rong Wu, Alteration in metastasis potential and gene expression in human lung cancer cell lines by ITGB8 silencing, *Anat. Rec.* 295 (2012) 1446–1454.
- [12] C.D. Chen, C.L. Wang, C.J. Yu, K.Y. Chien, Y.T. Chen, M.C. Chen, Y.S. Chang, C.C. Wu, J.S. Yu, Targeted proteomics pipeline reveals potential biomarkers for the diagnosis of metastatic lung cancer in pleural effusion, *J. Proteome Res.* 13 (6) (2014) 2818–2829.
- [13] J.S. Munger, D. Sheppard, Cross talk among TGF- $\beta$  signaling pathways, integrins, and the extracellular matrix, *Cold Spring Harb. Perspect. Biol.* 3 (2011)a005017.
- [14] T. Kadono, Y. Soma, K. Takehara, H. Nakagawa, Y. Ishibashi, K. Kikuchi, The growth regulation of neurofibroma cells in neurofibromatosis type-1: increased responses to PDGF-BB and TGF- $\beta$ 1, *Biochem. Biophys. Res. Commun.* 198 (3) (1994) 827–834.
- [15] N. Arase, A. Takeuchi, M. Unno, S. Hirano, T. Yokosuka, H. Arase, T. Saito, Heterotypic interaction of CRTAM with Necl2 induces cell adhesion on activated NK cells and CD8<sup>+</sup> T cells, *Int. Immunol.* 17 (9) (2005) 1227–1237.
- [16] J.P. Brosseau, D.C. Pichard, E.H. Legius, P. Wolkenstein, R.M. Lavker, J.O. Blakeley, V.M. Riccardi, S.K. Verma, I. Brownell, L.Q. Le, The biology of cutaneous neurofibromas: consensus recommendations for setting research priorities, *Neurology* 91 (2) (2018) S14–S20.
- [17] Manas Kotepui, Charin Thawornkuno, Porntip Chavalitshewinkoon-Petmitr, Phaibul Punyarit, Songsak Petmitr, Quantitative real-time RT-PCR of *ITGA7*, *SVEP1*, *TNS1*, *LPHN3*, *SEMA3G*, *KLB* and *MMP13* mRNA expression in breast cancer, *Asian Pac. J. Cancer Prev.* 13 (2012) 5879–5882.
- [18] Akira Orimo, Piyush B. Gupta, Dennis C. Sgroi, Fernando Arenzana-Seisdedos, Thierry Delaunay, Rizwan Naeem, Vincent J. Carey, Andrea L. Richardson, Robert A. Weinberg, Stromal fibroblasts present in invasive human breast carcinomas promote tumor growth and angiogenesis through elevated SDF-1/CXCL12 secretion, *Cell* 121 (2005) 335–348.
- [19] I. Shur, E. Zember-tov, R. Socher, D. Benayahu, SVEP1 expression is regulated in estrogen-dependent manner, *J Cell. Physiol.* 210 (2007) 732–739.
- [20] P.A. Guerrero, J.H. Tchaicha, Z. Chen, J.E. Morales, N. McCarty, Q. Wang, E.P. Sulman, G. Fuller, F.F. Lang, G. Rao, J.H. McCarty, Glioblastoma stem cells exploit the  $\alpha$ v $\beta$ 8 integrin-TGF $\beta$ 1 signaling axis to drive tumor initiation and progression, *Oncogene* 36 (47) (2017) 6568–6580.
- [21] F. Colland, X. Jacq, V. Trouplin, C. Mougou, C. Groizeleau, A. Hamburger, A. Meil, J. Wojcik, P. Legrain, J.M. Gauthier, Functional proteomics mapping of a human signaling pathway, *Genome Res.* 14 (7) (2004) 1324–1332.
- [22] Y. Zhang, X.H. Feng, R. Derynck, Smad3 and Smad4 cooperate with c-Jun/c-Fos to mediate TGF- $\beta$ -induced transcription, *Nature* 394 (6696) (1998) 909–913.
- [23] J.A. Markovics, J. Araya, S. Cambier, D. Jablons, A. Hill, P.J. Wolters, S.L. Nishimura, Transcription of the transforming growth factor beta activating integrin beta8 subunit is regulated by SP3, AP-1, and the p38 pathway, *J. Biol. Chem.* 285 (32) (2010) 24695–24706.